Cell-Surface Receptors and Proteins on Platelet Membranes Imaged by Scanning Force Microscopy Using Immunogold Contrast Enhancement

Steven J. Eppell,* Scott R. Simmons,‡ Ralph M. Albrecht,‡ and Roger E. Marchant*

*Department of Biomedical Engineering, Case Western Reserve University, Cleveland, Ohio 44106-7207, and ‡Department of Animal Health and Biomedical Sciences, University of Wisconsin, Madison, Wisconsin 53706-1581 USA

ABSTRACT   High resolution scanning force microscope (SFM) images of fibrinogen-exposed platelet membranes are presented. Using ultrasharp carbon tips, we are able to obtain submolecular scale resolution of membrane surface features. Corroboration of SFM results is achieved using low voltage, high resolution scanning electron microscopy (LVHRSEM) to image the same protein molecule that is seen in the SFM. We obtain accurate height dimensions by SFM complemented by accurate lateral dimensions obtained by LVHRSEM. The use of 14- and 5-nm gold labels to identify specific membrane-bound biomolecules and to provide contrast enhancement with the SFM is explored as a useful adjunct to observation of unlabeled material. It is shown that the labels are useful for locating specific protein molecules on platelet membrane surfaces and for assessing the distribution of these molecules using the SFM. Fourteen nm labels are shown to be visible over the membrane corrugation, whereas 5-nm labels appear difficult to resolve using the present SFM instrumental configuration. When using the 5-nm labels, collateral use of LVHRSEM allows one to examine SFM images at submolecular resolution and associate function with the structures imaged after the SFM experiment is completed.

INTRODUCTION

The horizon of biological surface research has been extended considerably by the introduction of the scanning force microscope (SFM). The ability to image exclusively the surface of an uncoated object with subcellular or even submolecular resolution and the potential to do this under water has stimulated a flurry of activity from the scientific community. This has resulted in significant advances in obtaining structural information of biologically relevant systems at the molecular (Horber et al., 1992; Parpura et al., 1993) and sub-molecular level (Weisenhorn et al., 1990; Emch et al., 1992; Arakawa et al., 1992; Lacapere et al., 1992; Allen et al., 1993). However, progress toward new understanding of the function of the systems under study has not been commensurate with this activity. One reason for this is that the SFM is indiscriminate in its contrast mechanism with respect to chemical composition and biological function. All features of a surface are recorded with approximately equal facility. Thus, a membrane receptor appears as a feature of about the same size as an adsorbed protein, which is a feature about the same size as a fold in the bilipid layer. As an example of the contrast problem with the SFM, we present a result from our studies on the interaction of blood plasma proteins with polymer surfaces. We began this study by looking at a bare polymer surface, low density polyethylene (NHLBI Standard) and at a glycoprotein, von Willebrand Factor, adsorbed on a surface of known topography, mica (Fig. 1). It is evident from this figure that if the protein were to be placed on top of the polymer, the protein would be lost in the topography of the polymer. This same situation is present when trying to image biomolecules on cell membranes.

To distinguish a specific biomolecule on a cell membrane surface by SFM, it is necessary either to use some complementary technique that provides additional information or to treat the surface or process the data in some way so as to make the various molecular components distinguishable. Some method for identifying the proteins and enhancing the contrast of the image in the region where the protein adsorbs is needed. In this report, we describe a study of cell-surface receptors and proteins on a blood platelet membrane imaged by SFM. We explore the use of carbon tips to enhance SFM resolution, the use of low voltage, high resolution scanning electron microscopy (LVHRSEM) to obtain complementary information, and the use of 14- and 5-nm gold bead labels to locate and identify specific glycoproteins on the platelet membrane. Although both SFM and LVHRSEM have theoretical resolution limits well into the submolecular regime, there exist vagaries of the two techniques that result in image contrast that is unrelated to topography. By using both SFM and LVHRSEM in a correlative way, we are able to focus on objects that appear in both microscopes and are thus less likely to be imaging artifacts. This leads to a more complete picture of the surface and more confidence concerning the topographic aspects of our data than is possible with either technique alone.

In addition to using complimentary imaging techniques, we have examined fibrinogen on platelet membranes by modifying the surface to selectively enhance the contrast of a region based on its biological function. This is accomplished by using the immunogold labeling technique (Roth, 1983; Park et al., 1986). The gold bead labels provide contrast enhancement of the SFM and allowed the labeled glycoproteins to be distinguished from the background molecular scale features of the platelet membrane. We used the colloidal gold technique for several reasons. It was a well
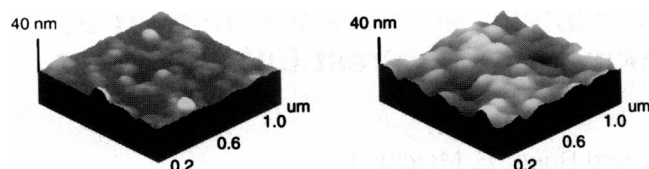
FIGURE 1   (a) SFM image of von Willebrand Factor deposited on freshly cleaved mica. The protein, isolated and purified as described previously (Marchant, 1992), was dissolved in ammonium acetate and then deposited on the mica. (b) SFM image of NHLBI standard low density polyethylene displayed using parameters identical to the vWF image in a.

established technique in electron microscopy, it allowed us to compare our SFM results with electron micrographs of the same surface, and it provided a range of contrast enhancement based on a range of gold label sizes. Previously, we have used colloidal gold labeling to investigate the binding of fibrinogen molecules to receptors on platelet surfaces and the subsequent movement of the ligand/receptor complexes on the membrane surfaces (Albrecht et al., 1989). Images of the colloidal gold labels were obtained utilizing correlative video-enhanced light microscopy, high voltage transmission electron microscopy, and LVHRSEM. The recently reported application of this technique, using relatively large immunogold labels of 30-nm diameter to provide contrast enhancement in SFM topographs of lymphocytes, is novel and shown to be quite useful (Putnam et al., 1993).

In this paper, we extend the use of immunogold labels in the field of SFM. To test the feasibility of this approach, we needed to visualize the same molecule with the SFM and the LVHRSEM. This allowed us to develop confidence that we were actually visualizing the gold beads with the SFM. The membrane of a blood platelet is irregular on a micron scale, so that by supporting the platelet on an electron microscope finder grid, we obtained a surface that provided easy scaling from a sub-millimeter down to a nanometer dimension. Collateral studies with LVHRSEM then confirm that we have been successful in enhancing the SFM contrast based on biological function. Further, we have been successful in imaging exactly the same glycoprotein molecules and gold labels in the SFM and the LVHRSEM.

MATERIALS AND METHODS

Sample preparation

As we have detailed previously (Loftus et al., 1984; Olorundare et al., 1993), platelets adherent to formvar-filmed finder grids were labeled with fibrinogen or IgG antibody to the fibrinogen receptor, either soluble or gold conjugated (monoclonal antibody against the platelet fibrinogen receptor 10E5 was a generous gift from Dr. Barry Coller, State University of New York, Stony Brook). Labeled platelets were prepared for electron microscopy by glutaraldehyde and osmium fixation, ethanol dehydration, and drying by the critical point method (Albrecht et al., 1993, 1992). Fibrinogen was purified from fresh or frozen plasma by precipitation with 25% saturated ammonium sulfate followed by DEAE-cellulose chromatography (Mosher, 1975). The specimen was then sputter-coated with 1–2 nm of platinum.

Electron microscopy

Samples were imaged in a Hitachi S-900 low voltage, high resolution scanning electron microscope (LVHRSEM) (Integrated Microscopy Resource, University of Wisconsin, Madison) at 1–3 kV accelerating voltage (V_0) in the secondary electron (SE) mode, providing a topographical image of the surface, or at 4–10 kV in the backscattered electron (BSE) mode for identification of gold labels. This LVHRSEM has a field emission probe as well as low aberration lenses, allowing it to obtain a narrow electron beam at low V_0. This combination of small probe size at low V_0 permits examination of biological material at high resolution with low beam penetration, producing images of cell surfaces of such resolution and contrast that visualization of individual protein molecules directly on the cell surface membrane is possible. At low V_0, gold labels can be identified by their shape but cannot be distinguished from other cell surface features of similar size and shape. Increasing V_0 to 3–5 kV and above increases beam penetration, progressively decreasing the amount of surface detail in the image but making possible positive identification of gold labels through atomic number (z) contrast. The use of backscattered electrons for imaging further increases differences in z contrast. BSE detectors using the YAG-type scintillator (Autrata) provide very high sensitivity such that BSE imaging of gold labeled cell surfaces at lower beam voltages permits positive identification of gold labels down to 1 nm in size and a concomitant increase in the amount of surface detail in the image as the voltage is decreased (Pawley et. al, 1988; Autrata, 1989).

Scanning force microscopy

All samples were imaged under ambient air conditions with a Digital Instruments Nanoscope III SFM (Center for Cardiovascular Biomaterials, Case Western Reserve University, Cleveland, OH). Commercial Si_3N_4 tips integrated on Si_3N_4 cantilevers (Nanoprobes, Digital Instruments, Santa Barbara, CA) were used. Various triangularly shaped cantilevers were used. Some were 100 μm long with a manufacturer's reported spring constant of 0.6 or 0.4 N/m. Others were 200 μm long with a manufacturer's reported spring constant of 0.1 N/m. The tips were pyramidally shaped and ~5 μm tall. Some of the images were collected using an ultrasharp carbon spike grown on top of the silicon nitride pyramid (Akama et al., 1990; Kam et al., 1991; Keller et al., 1992). These spikes were grown by first soaking the entire cantilever assembly in EM grade acetone and then exposing the apex of the Si_3N_4 tip to a stationary focused beam at 20–25 kV accelerating voltage for ~2 min in the S-900 SEM. We did have difficulty reproducibly forming the carbon spikes with this procedure. We suspect that an adventitious contaminant on the inside surface of the beaker of acetone was responsible for the successfully grown tips. Typical engagement forces were ~10 nN as determined by multiplying the cantilever spring constant by the distance the cantilever was flexed between its setpoint and the point at which it was flexed when tip and surface were >5 μm apart. Unless otherwise stated, all SFM images reported below were taken in the constant force mode. In this mode of operation, a digital feedback loop uses the position of a focused laser beam (which is reflected off the back of the cantilever and onto a split photodiode) as its input and voltage to the z-piezo as its output to maintain a constant laser beam position. This requires that a set point position be chosen for the laser beam. We chose for this set point the position that the laser beam assumes when the tip and sample surface are far apart (>5 μm). During the course of scanning, the setpoint drifted resulting in the typical engagement forces of ~10 nN as mentioned above.

RESULTS AND DISCUSSION

Fig. 2 shows a gallery of images of a platelet. The images are paired with the LVHRSEM data presented on the left and the SFM data presented on the right. These images were collected using a carbon tip deposited on a Si_3N_4 pyramid. Fig. 2, a and b show that the same platelet has been located in both microscopes. A successive series of increasing magnification

changes were made. At first, a portion of the platelet edge was kept in view to provide a reference (Fig. 2, c and D). When objects on the platelet membrane became large enough, they were used as fiduciary marks for probing regions of the membrane closer to the center of the platelet (Fig. 2, e and f). Notice that in Fig. 2, e and f the gross features are the same in both SFM and LVHRSEM data; the features labeled 1–4 (see Fig. 3) are easily recognizable in both images. It is also evident that the LVHRSEM data appear sharper and of higher lateral resolution than the SFM data. For example, feature 1 has a measured width of 29 nm in the LVHRSEM data and a measured width of 81 nm in the SFM data. This broadening of the image data by SFM has been reported and explained previously (Thundat et al., 1992; Bustamante et al., 1992; Eppell et al., 1993). The broadening effect caused by the finite size of the tip is substantially reduced, but not eliminated, by using a carbon tip rather than the standard commercial Si_3N_4 tip. The most accurate data are obtained using the SFM to provide accurate height information complemented by high resolution lateral information from the LVHRSEM.

The height of feature 1, which is not known by LVHRSEM, is measured by SFM as 30 nm. This object along with features 2–4 could be from a number of sources. A case can be made that these objects are comprised of fibrinogen. Fibrinogen bound to spread platelets exhibits a strong tendency to form small aggregates. These aggregates can be clearly visualized in LVHRSEM of platelet surfaces (Albrecht et al., 1988). Although individual fibrinogen molecules are large enough to be resolved in the LVHRSEM and the SFM, the complexity and roughness of the platelet surface make it difficult to distinguish individual bound molecules from background corrugation. Fig. 2, e and f show a region of a spread platelet surface on which a number of small aggregates and individual molecules are bound. We have convincing evidence that the features discussed in Fig. 2 are fibrinogen aggregates based on LVHRSEM studies comparing exogenous fibrinogen-treated platelets with untreated platelets (S. R. Simmons et al., unpublished data). The aggregates appear as light gray branched or globular structures that, although easily visualized by LVHRSEM or SFM, cannot be positively identified without some means of contrast enhancement such as colloidal gold labeling. Based solely on these LVHRSEM and SFM data, these branched and globular structures could be aggregates of fibrinogen or some other protein, could represent an early stage of vesiculation or of microparticle formation, or could simply arise from the normal corrugation or roughness of the platelet surface. If we are looking for features that represent single bound fibrinogen molecules or single membrane receptors, we must look for objects that are 5–10 times smaller in height than these apparent protein aggregates (c.f. features 5–8 in Fig. 2 f).

Single fibrinogen molecules have been visualized in transmission electron micrographs of rotary shadowed or negatively stained preparations as three interconnected globular domains each 5–6 nm in diameter in a rod-shaped molecule

45–47 nm long. A number of rod shaped structures of this approximate length can be seen in the LVHRSEM image of the platelet surface. Our SFM data show that these structures are around 7 nm in height, consistent with these features being fibrinogen molecules. The trinodular structure of the fibrinogen molecule cannot be distinguished in either the SFM or LVHRSEM images of the structures. This may be due to contributions to the image from other surrounding or underlying structures, such as the glycoprotein receptor to which the fibrinogen molecule is bound. An alternative explanation is that the conformation of the molecule when bound to its receptor in a physiological buffer is such that the three domains of the molecule are not separated from one another as they are when spread on a flat surface or embedded in uranyl acetate. Other features in the LVHRSEM image appear as round, 12–13 nm diameter particles, consistent with these being glycoprotein receptors (Weisel et al., 1992). These particles also can be seen by SFM to protrude ~7 nm from the membrane surface. Feature 7 has a diameter of 13 nm measured on the SEM negative and a height of 7 nm as measured by SFM. This also fits with this object being a membrane receptor.

The resolution of the features in Fig. 2 f is about twice as high as that in the succeeding images, which were collected with Si_3N_4 pyramids that did not have carbon spikes. Thus, features with dimensions equivalent to individual globular domains of adsorbed fibrinogen molecules can be resolved here but not in the succeeding images. It should be noted that this is not a general result with respect to Si_3N_4 pyramidal tips. The pyramidal tips vary considerably in their geometry and some tips are capable of resolving individual domains. However, this is not possible with all or even most Si_3N_4 pyramidal tips.

Although the above discussion of Fig. 2 shows complementary data obtained from collateral SFM and LVHRSEM images, it is still speculative because of the lack of functional specificity. There are many features in both the SFM and LVHRSEM images, and by selectively focusing on particular regions one can find corroboration for many different hypotheses. To eliminate ambiguities in the identification of molecular features, it is necessary to find a technique for positively identifying the objects of interest. This problem has been solved in part for scanning electron microscopy. Immunogold labeling has been used for just such a purpose for several years and by a number of research groups (Roth, 1983; Park et al., 1986; Simmons et al., 1990; Murthy et al., 1987; Park et al., 1987; Herrera, 1992; Stirling, 1990; Horisberger, 1979). The use of colloidal gold to aid in SFM studies has recently been suggested (Shaiu et al., 1993; Vesenka et al., 1993). However, the main thrust of these papers has been to use the gold as a size calibration standard. Putman et al. (1993) have shown that immunogold labeling does show promise as a contrast enhancement mechanism in SFM. They used immunogold-labeled lymphocytes to show that 30-nm gold labels provide contrast enhancement of SFM topographs. We will show that colloidal gold can also be used to enhance the ability to identify specific features in SFM
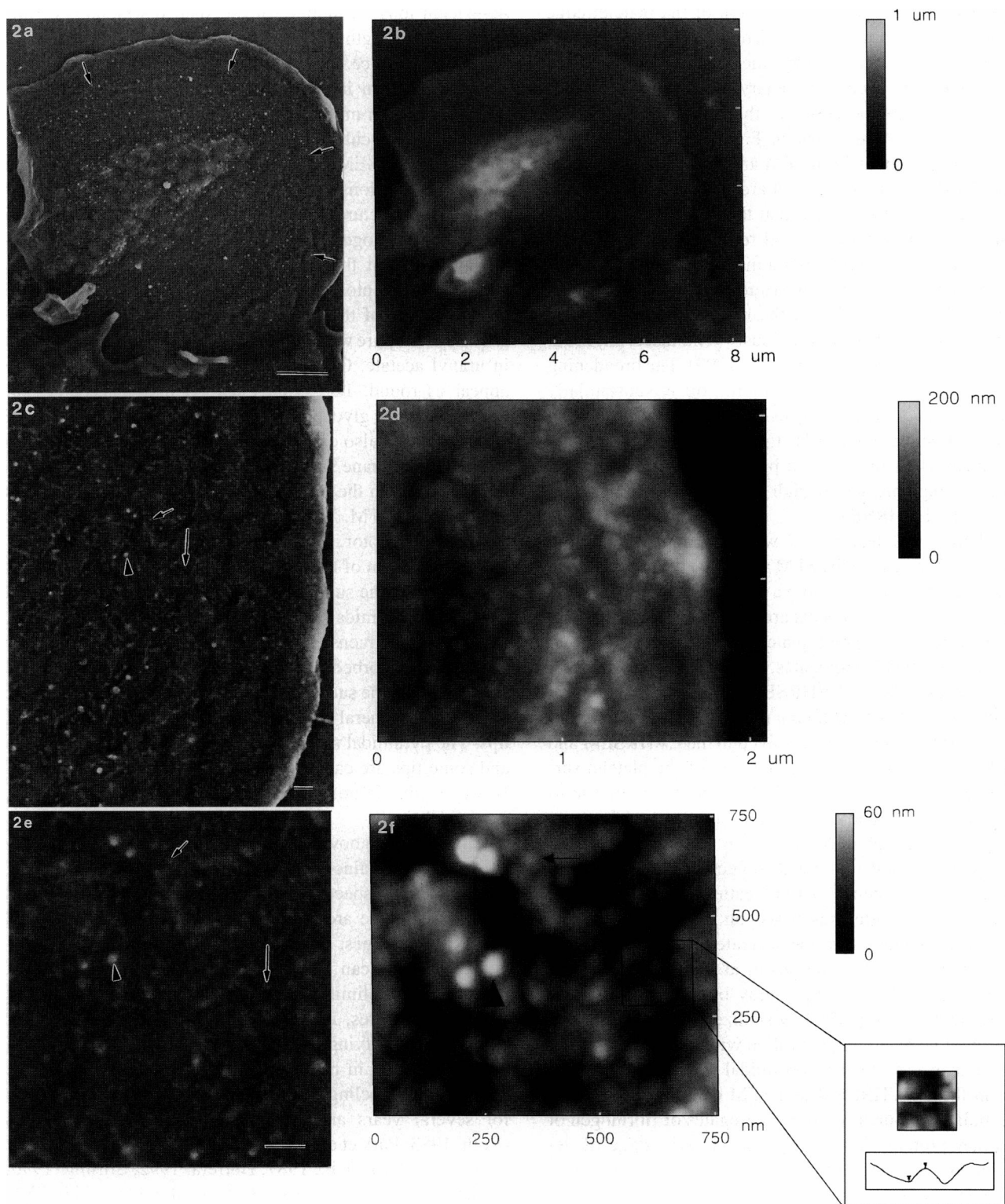
FIGURE 2   LVHRSEM. Surface adherent, spread platelet on formvar filmed finder grid. Image taken at 3-kV accelerating voltage shows primarily surface detail, with very little beam penetration. Specimen coated with 1–2 nm platinum. The platelet was fixed 5 min after addition of exogenous fibrinogen. Centripetal translocation of bound fibrinogen has left the membrane near the platelet perimeter free of fibrinogen. Small aggregates of bound fibrinogen (*arrows*) have begun to form the characteristic band on the platelet surface surrounding the granulomere. Bar = 1 μm. (*b*) SFM image of the same platelet shown in *a*. The SFM data show that the perimeter of the platelet membrane is ~100 nm above the formvar film and the granulomere is 300–350 nm above the perimeter of the platelet. (*c*) LVHRSEM. Increased magnification of platelet shown in *a*. Larger aggregates of protein appear as bright objects on the membrane surface (*arrowhead*). Smaller branched and globular protein aggregates appear as dimmer gray features (*small arrow*). The aggregates have formed as fibrinogen bound to platelet surface receptors is translocated centripetally, leaving the platelet perimeter free of bound fibrinogen. Small particles in platelet membrane at perimeter are of appropriate size for integral membrane glycoprotein receptors (*large arrow*). Bar = 0.1 μm. (*d*) SFM of region shown in *c*. The intensity of features near the membrane perimeter does not decrease as it does in the LVHRSEM image (*c*). (*e*) LVHRSEM. Increased magnification
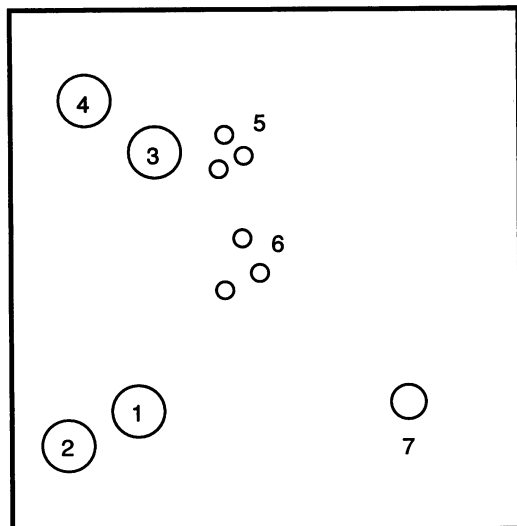
FIGURE 3 Schematic drawing of a few of the features in Fig. 2, *e* and *f*. Feature 1 = big arrow head; Feature 5 = short arrow; Feature 7 = long arrow.

images of platelet membranes. In addition to using the immunogold technique, we will show that direct conjugation of the gold label to the protein of interest also provides contrast enhancement with the SFM. Through the collateral use of the LVHRSEM, we will prove that the contrast enhancement is correlated with the gold labels in a one-to-one fashion. Finally, we will show that there is currently a lower limit to the usable size of the gold labels with present SFM technology.

The contrast enhancement provided by immunogold labels results in part from different mechanisms between SFM and LVHRSEM. With the LVHRSEM, enhancement occurs both because of the round regular shape and perhaps more importantly because the gold label is electron dense. Thus, it provides a site for enhanced backscatter and secondary emission of electrons. This causes the gold particle to look like a bright star in a gray sky when it is imaged against a mostly carbon background. In SFM, the gold label sticks out because of its well defined geometry and size and perhaps its low compressibility. The SFM operator looks at a relatively irregular surface and tries to locate a well defined roughly spherical cap. Once this is identified, a careful search is performed around the gold label to see if the biomolecule that is attached to it is visible.

Immunogold labeling

Our SFM and LVHRSEM data show high resolution down to molecular scales but lack the means for molecular iden-

tification. To address this problem, we began by conjugating fibrinogen receptor antibodies to 14-nm gold particles (Loftus et al., 1984; Olorundare et al., 1993). These coated particles were then allowed to bind to receptors on spread platelets that had been deposited on formvar-coated EM finder grids. Fig. 4 shows LVHRSEM and SFM images of a surface adherent platelet that had been prepared in this manner. The overall shape of the platelet is convincing evidence that the same platelet has been imaged by the two techniques. It is obvious from the LVHRSEM image (Fig. 4 *a*) that the surface of the platelet has been labeled by the fibrinogen gold conjugates. When displaying the SFM data with a *z* range large enough to show the full platelet, it is not apparent that the gold conjugates have been sensed by the SFM tip (Fig. 4 *b*). However, if a small portion of the image is selected and a *z* range more appropriate for visualization of the conjugates is chosen, then it becomes apparent that the SFM tip is indeed sensing the gold beads (*inset* in Fig. 4 *b*). Although the lateral resolution of the LVHRSEM data is better than the SFM data, the height information from the SFM gives a good complementary view of the surface. For example, the SFM shows that the central granulomere is about 500 nm higher than the rest of the platelet membrane. Also, there are a few tall objects in the membrane that show up quite well in the SFM image but are not so clear in the LVHRSEM image.

Fig. 4, *c* and *d* show magnified images of the lower right portion of the platelet indicated by the arrow in Fig. 4 *a*. At this scan size, the labels are quite obvious in the SFM data as well as the LVHRSEM data. At higher accelerating voltage (4 kV, BSE mode), the LVHRSEM data reflect the size of the gold labels without their protein coat. The width of the labels, measured from the negatives, is 14–21 nm. At low accelerating voltage (1.5 kV), the LVHRSEM data reflect the label with its protein coat. At 1.5 kV, the LVHRSEM label widths are 26–34 nm. The SFM data show the labels to have an average height of 22.9 ± 5.8 nm (N = 23) and average diameter of 53 ± 6.3 nm (N = 23). If we assume that the labels are spherical, the height of the labels imaged by SFM should correspond to the width of the low voltage LVHRSEM labels. Within the error of our measurements, there is good agreement between the two techniques.

With these 14-nm gold labels, the SFM can be used to map out the distribution of fibrinogen receptors on the platelet surface. We are in the process of duplicating this result in vitro. Success in this endeavor will allow us to augment the enhanced video microscopy studies of receptor distribution and motion reported previously (Albrecht et al., 1989). Although this type of study is useful, we have not succeeded

---

of region shown in *c* and *d*. Large bright aggregates (*arrowhead*) and gray globular or branched protein aggregates (*small arrow*) can be seen, as well as structures of the approximate size and shape of individual fibrinogen molecules or platelet surface receptors (*large arrow*). Arrows indicate same structures as in *c* and *d*. Bar = 0.1 μm. (*f*) SFM of region shown in *e*. Arrows indicate same structures as in *c–e*. Both the LVHRSEM and the SFM provide images in which molecular-scale structures can be visualized. Although lateral dimensions of objects in this size range are inflated in SFM images, the SFM gives accurate *z* axis information. The length between the cursors on the line scan in the inset is 23 nm. The vertical distance between the cursors is 6.7 nm. This height along with the diameter measured from the SEM negative of E demonstrates that this is a membrane particle of appropriate dimensions to be a glycoprotein receptor.
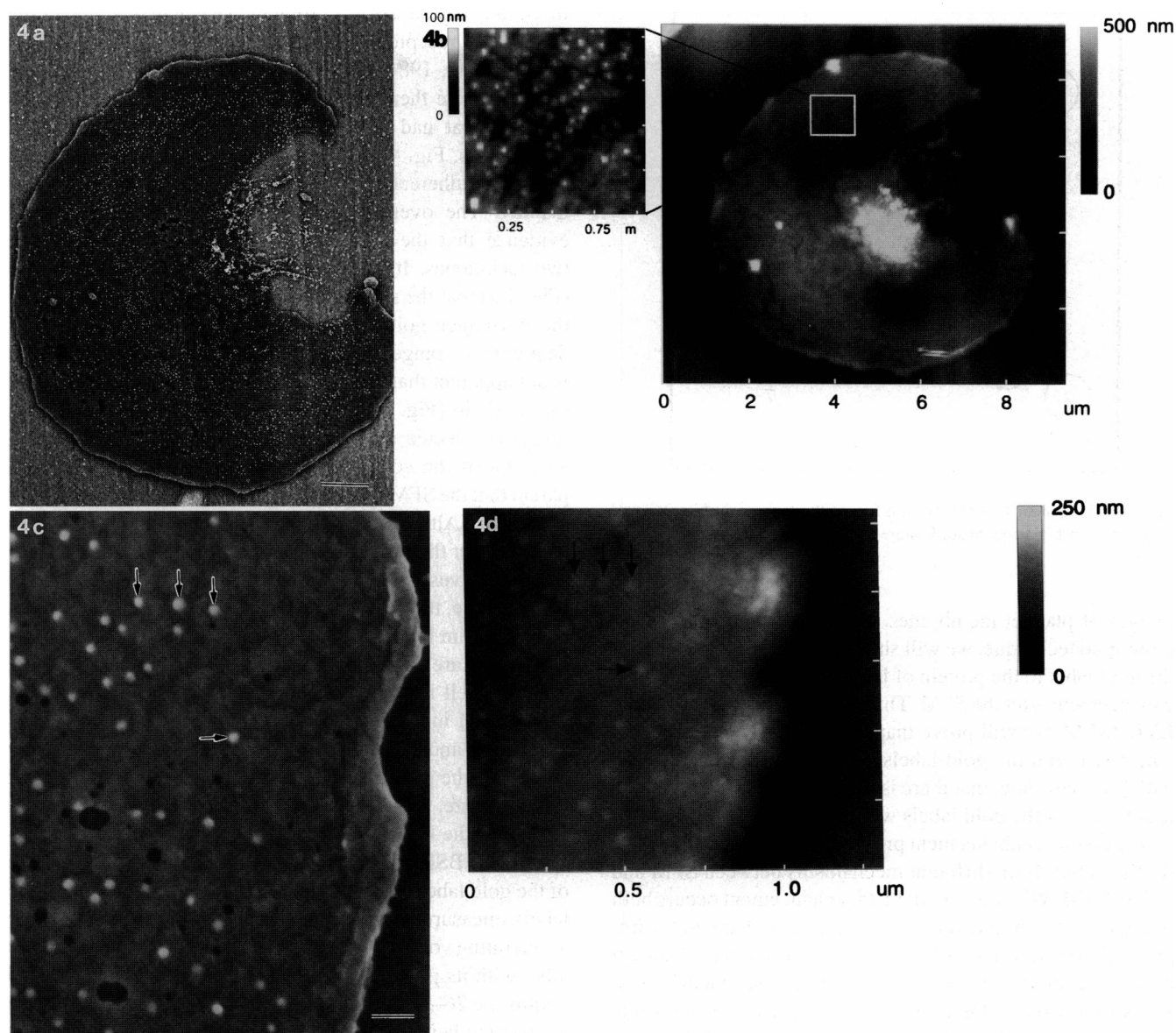
FIGURE 4 (*a*) LVHRSEM image of spread platelet labeled with 14-nm colloidal gold particles conjugated to IgG antibody to the platelet fibrinogen receptor. The image was taken in the backscattered electron imaging mode at 4.0-kV accelerating voltage. The gold labels appear as small white dots covering the platelet surface. Bar = 1.0 μm. (*b*) SFM image of same platelet as in Fig. 3 *a*. Although the gold labels are not readily seen in the SFM image at this magnification, the inset shows that, with the appropriate choice of *z* range, the SFM data do contain the information to show the gold labels. (*c*) LVHRSEM. Increased magnification of platelet shown in *a*. Image taken in the secondary electron imaging mode at 1.5-kV accelerating voltage. Beam penetration at this low voltage is slight, such that the surface of the protein coating on the gold labels (*arrows*) is seen, making possible a direct comparison of the sizes of the gold labels in the SFM and LVHRSEM images. Holes in the platelet membrane are probably due to drying during sample preparation. Bar = 0.1 μm. (*d*) SFM of same region of platelet surface as shown in Fig. 3 *c*. Arrows indicate same gold labels as in Fig. 3 *c*. Although the diameters of the labels in the SFM image are approximately twice that of the diameters as measured from the LVHRSEM image, the heights of the labels in the SFM data are in the same range as the diameters in the LVHRSEM, as is appropriate for roughly spherical particles. Many of the holes in the membrane seen by LVHRSEM (*c*) are also apparent in this SFM image.

in enhancing our ability to obtain detailed images of the ultrastructure of the membrane surface. The 14-nm gold labels are too large; they occlude our view of the feature of interest on the surface. The next logical step was to reproduce this experiment using a smaller gold label. We have done this using 5-nm gold conjugated directly to fibrinogen.

The 5-nm conjugates are quite different from the 14-nm conjugates. With the 5-nm labels, each protein conjugates to

one or more labels (Simmons, 1989). Thus, the labels can be used to show the orientation of the protein as well as to show its distribution. It is less clear when using the 5-nm labels to see where the SFM data agree with the LVHRSEM data compared with the 14-nm labels. There are two reasons for this. First, the label height is equal to or smaller than the protein height. Thus, there is not much contrast enhancement with the SFM. Second, the Si_3N_4 SFM probe tip is too broad

to distinguish between the E and D domains of the fibrinogen on this rough substrate. Thus, images that appear as doublets and triplets of gold label in the LVHRSEM data appear as single objects in the SFM data. However, if one picks a fiduciary feature on the surface that is obvious in both the SFM and LVHRSEM image and uses the distance measured from this mark to locate other smaller features on the surface, one can find strong corroboration between the SFM and LVHRSEM data.

Fig. 5 shows a LVHRSEM image of a platelet membrane coated with fibrinogen that has been conjugated to 5-nm gold particles. Fig. 6 shows an SFM image of the same region. Fig. 7 shows a schematic drawing of a few of the features on this surface. The results of measurement of these features using the SFM data are presented in Table 1. The data in this table were collected using line scans like those shown in Fig. 6 d. Fig. 6 d also shows a high resolution scan of features 4, 5, and 6 (cf. Fig. 7). Notice that the fibrinogen molecules are sitting in a depression in the membrane. In addition to a large depression that extends across the entire image, each individual molecule is sitting in its own small depression. This may be due to shrinkage of the platelet resulting from the drying procedure. Another explanation is that the molecules were tightly bound to the platelet cytoskeleton while they moved from the platelet periphery to final positions on the surface surrounding the granulomere. This tight binding could cause a small depression in the membrane surrounding the bound molecule.

The height of features 4, 5, and 6 ranged from 10 to 18 nm depending on what angle the cross section was taken at and which side of the feature the baseline was selected. All of the heights were greater than the 3–6 nm value expected for a single fibrinogen molecule. This may be due to the presence of the membrane receptor below the fibrinogen. The receptor in conjunction with folds in the bilipid layer may account for the added height measured by the SFM. It is also possible that, although the 5-nm labels are not obvious in the image, they have caused the measured height of the molecules to increase. With sharper SFM tips, this theory could be tested more directly.

Notice that features that are distinct domains in the LVHRSEM image appear as single domains in the SFM image. A very clear example of this is seen in features 4, 5, and 6. These are probably three separate fibrinogen molecules, each with two labels. The SFM shows not three domains, or even two domains, for each of these molecules. Instead, only
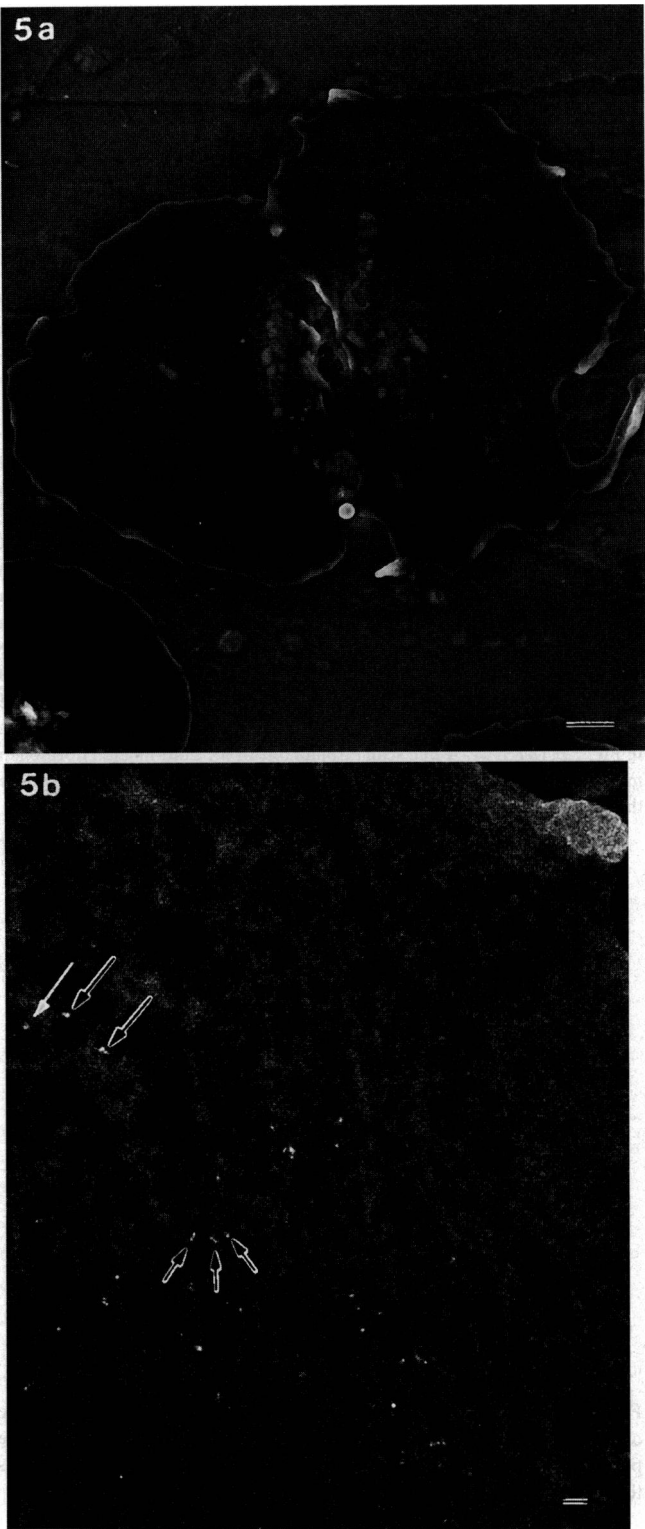
TABLE 1   Dimensions of surface features from Fig. 6 C

#	Height	Width (long axis)	Width (short axis)
1	20	88	77
2	25	84	81
3	24	86	86
4	13	70	54
5	11	74	54
6	12	68	54

The feature #s are indicated in Fig. 7.

FIGURE 5   (a) LVHRSEM. Pair of spread platelets labeled with fibrinogen conjugated to 5-nm colloidal gold particles. Bar = 1 μm. (b) LVHRSEM backscattered electron image. Increased magnification of platelet shown in a. Larger aggregates of fibrinogen molecules (large arrows) are used as fiduciary marks for locating smaller objects on the surface. Each fibrinogen molecule, conjugated to one or several of the small gold particles, is bound to receptors on the platelet surface. Note that the three molecules indicated by small arrows each are bound to two or three gold labels. Bar = 0.1 μm.
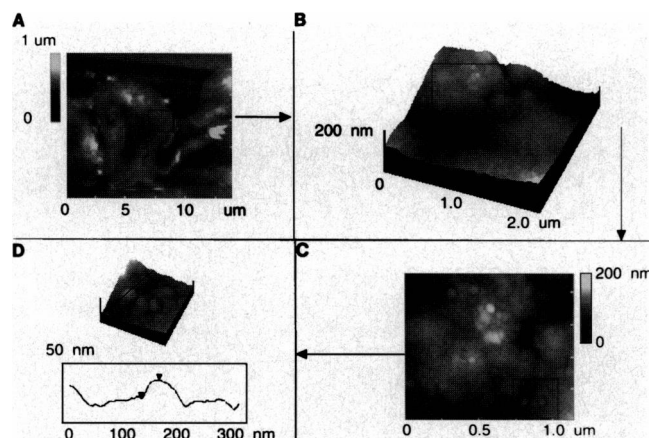
FIGURE 6 (a) SFM. Low magnification showing outline and general topography of the same platelet seen in Fig. 5 a. (b) SFM. Higher resolution scan of the area shown in Fig. 5 b. The z axis is slightly exaggerated to show the degree of roughness of the platelet surface. It is evident that the platelet membrane is increasing in height from its perimeter (*lower right corner*) toward its granulomer (*upper left corner*). (c) SFM. This image is drawn from the same data set as b. The magnification was performed after data collection. The same set of three large features (*large arrows*) is found here as was seen in the LVHRSEM image (Fig. 5 b). The box is located ~860 nm down and ~500 nm to the right of the set of three large features. The box contains the same three fibrinogen molecules indicated by small arrows in Fig. 5 b. (d) SFM. A line scan through one of the gold-labeled fibrinogen molecules shows the height above the surface to be 13 nm, slightly more than expected for an unlabeled fibrinogen molecule.
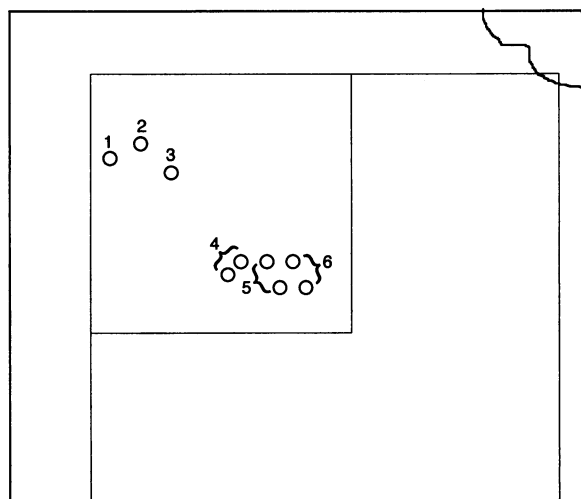

FIGURE 7 Schematic drawing of a few of the features seen on the surface of the platelet displayed in Figs. 5 and 6. The outer box represents the perimeter of Fig. 5 b and the SFM image in Fig. 6 b. The inner box represents the perimeter of the SFM image shown in Fig. 6 c.

one domain per pair is seen. Also, notice that the labels do not cause the labeled fibrinogen to stick out with enhanced contrast over the unlabeled regions of the surface. There are objects in the SFM data of similar size that have no corresponding bright spot in the LVHRSEM image. This demonstrates that the 5-nm gold conjugates are not useful in terms of enhancing contrast in SFM experiments in this protein/receptor system given the present capabilities of the

SFM. However, with only the SFM data to analyze, one would be very hard pressed to find features 4, 5, and 6. And once this area was isolated, one would be justifiably skeptical that they were indeed fibrinogen molecules. Using the LVHRSEM collaterally with the SFM data, and triangulating off of larger features like 1, 2, and 3 that are obvious in both images, one can easily locate the regions of interest in the SFM data and analyze those portions of the image more thoroughly, thus confirming the identity of the gold-labeled fibrinogen molecules (Albrecht et al., 1989; Loftus et al., 1984; Olorundare et al., 1993).

Implications for cell and protein studies by SFM

With the advent of submolecular resolution microscopies, the present challenge is to combine functional specificity with improvements in spatial resolution. With contact mode SFM, we found significant improvement in lateral resolution using ultrasharp carbon probe tips compared with standard Si_3N_4 tips. Recently, we determined through morphological image processing techniques that the carbon probe tips are more symmetric, sharper, have a higher aspect ratio, and introduce fewer artifacts than Si_3N_4 tips when imaging objects sized similarly to globular proteins (Wilson et al., 1995, in preparation). There is also some experimental evidence that these carbon probes are superior for imaging biological molecules compared with etched silicon tips that have similar radii of curvature (C. Bustamante, private communication).

We have demonstrated one way of introducing functional specificity by using gold labels either conjugated directly to the molecule of interest or attached to the molecule via an intermediary immunoglobulin fragment. Although this approach has been shown to be effective using labels significantly smaller than the imaged protein (5 nm or less) using SEM, our data show the same is not true for SFM. This suggests the need for further refinement in labeling or other modes of operation that would provide the SFM with sensitivity to labels on the submolecular scale of biopolymers (<10 nm).

One possible approach is to use compliance mode SFM. This mode takes advantage of the fact that the SFM is sensitive to more than just topography. Images include information dependent upon the material properties of the specimen such as its hardness and frictional coefficient. Artificially high points can be generated over regions of the surface that are harder than average. By imaging in the compliance mode, data can be obtained that reflect these changes in surface hardness. For example, compliance mode SFM would take advantage of both the shape and relative hardness of the gold labels compared with the biological surface. We have collected one preliminary image of a platelet membrane labeled with the 10E5-gold antibodies mentioned above. The contrast of the gold labels with respect to the rest of the platelet was significantly enhanced using the compliance mode. The future of this line of investigation looks promising. In addition, regions of the surface that are "stickier" than average can cause artificially high or low points depending on the scan direction. Again, this can be used to

advantage when imaging in the lateral force mode, in which case the data reflect the local coefficients of friction. It is only in the past year or so that these modes of operation have become standard in the SFM community. A problem that remains to be solved is how to distinguish unambiguously the topographic, frictional, and compliance contributions to an SFM image.

Another method for refining functionally specific SFM experiments will come from the exploration of novel labels. Application of near-field optical techniques in conjunction with SFM will alow for development of fluorescent labels to replace the relatively large gold markers. One can also envisage use of magnetic force microscopy with SFM leading to the development of magnetic marker particles. Perhaps the most powerful technique will emerge from the recently demonstrated method of fabricating functionalized SFM probe tips (Florin et al., 1994). This will lead to the use of forces involved in specific ligand-receptor interactions to provide a basis for image contrast providing collateral information to SFM topographic imaging. Thus, two desirable complementary techniques will be present in the same instrument.

The development of these techniques should reduce the present difficulties in fully utilizing the unique in vitro capability of the SFM. This will result in our ability to identify and image at submolecular resolution surface receptors and bound ligands while following processes such as receptor expression, movement, and organization on living cells. One may be confident that studies beyond the routine use of the SFM will depend not only on instrumental developments, but also on the innovative use of existing and novel sample preparation methods including novel labeling methods, utilization of immobilization methodologies, as well as the complimentary use of ultra high resolution optical and electron microscopy techniques. This will lead to a substantial extension of the horizon of biological research that will include concomitant progress in our understanding of structure-function relationships of cell surface molecules.

CONCLUSIONS

As demonstrated by the results we have presented, the SFM provides unique opportunities to visualize biological surfaces and biopolymers at the molecular level. With any technique, obtaining complimentary data is essential in overcoming the uncertainties and induced artifacts present in a single technique. Complementary techniques that provide images of a surface of similar resolution to the SFM are not plentiful. LVHRSEM is one such technique, and we have demonstrated how it can be used in a correlative way to provide a more complete picture of the surface than is obtainable with either technique alone. We have shown that SFM imaging of platelet surfaces using carbon tips provides images of such resolution as to permit visualization of individual protein molecules on the platelet surface membrane. Through the use of collateral LVHRSEM, we proved that the use of large enough gold labels conjugated to specific proteins of interest does result in contrast enhancement of SFM topographs over

the area where the labeled protein attaches to the surface. A 14-nm label is large enough to provide this contrast enhancement on a spread platelet membrane, whereas a 5-nm label is too small. The use of gold labeling in conjunction with collateral LVHRSEM imaging allows one to unambiguously identify features in the SFM images due to fibrinogen and fibrinogen receptor antibody from features due to other structures. This identification is possible using 5-nm gold labels and the relatively blunt tip of an Si_3N_4 probe.

REFERENCES

Akama, Y., E. Nishimura, and A. Sakai. 1990. New scanning tunneling microscopy tip for measuring surface topography. J. Vac. Sci. Technol. A. 8:429–433.

Albrecht, R. M., S. L. Goodman, and S. R. Simmons. 1989. Distribution and Movement of Membrane-Associated Platelet glycoproteins: use of colloidal gold with correlative video-enhanced light microscopy, low-voltage high-resolution scanning electron microscopy, and high-voltage transmission electron microscopy. Am. J. Anat. 185 :149–164.

Albrecht, R. M., O. E. Olorundare, and S. R. Simmons. 1988. Fibrinogen receptor movement in the surface membrane of adherent fully spread platelets. In Fibrinogen, Vol. III, Biochemistry, Biological Functions, Gene Regulation and Expression. M. Mosesson, D. Amrane, K. Sienbenlist, and J. Diorio, editors. Excerpta Medica, Elsevier, Amsterdam. 211–214.

Albrecht, R. M., O. E. Olorundare, S. R. Simmons, J. C. Loftus, and D. F. Mosher. 1992. Use of correlative microscopy with colloidal gold labeling to demonstrate platelet receptor distribution and movement. Methods Enzymol. 215:456–479.

Albrecht, R. M., S. R. Simmons, and J. B. Pawley. 1993. Use of correlative video enhanced light microscopy, high voltage transmission electron microscopy, and field emission scanning electron microscopy in the localization of colloidal gold labels. In Immunocytochemistry: A Practical Approach. J. Beesley, editor. Oxford University Press, Oxford. 151–174.

Allen, M. J., X. F. Daong, T. O'Neil, E. P. Yau, S. C. Kowalczykowski, J. Gatewood, R. Balhorn, and E. M. Bradbury. 1993. Atomic force microscopy measurements of nucleosomes cores assembled along defined DNA sequences. Biochemistry. 32:8390–8396.

Arakawa, H., K. Umemura, and A. Ikai. 1992. Protein images obtained by STM, SFM and TEM. Nature. 358:171–173.

Autrata, R. 1989. Backscattered electron imaging using single crystal scintillator detectors. Scanning Microsc. 3:739–763.

Bustamante, C., J. Vesenka, C. L. Tang, W. Rees, M. Guthold, and R. Keller. 1992. Circular DNA molecules imaged in air by scanning force microscopy. Biochemistry. 31:22–26.

Emch, R., F. Zenhausern, M. Jobin, M. Taborelli, and P. Descouts. 1992. Morphological difference between fibronectin sprayed on mica and on PMMA. Ultramicroscopy. 42:1155–1160.

Eppell, S. J., F. R. Zypman, and R. E. Marchant. 1993. Probing the resolution limits and tip interactions of atomic force microscopy in the study of globular proteins. Langmuir. 9:2281–2288.

Florin, E.-L., V. T. Moy, and H. E. Gaub. 1994. Adhesion forces between individual ligand-receptor pairs. Science. 264:415–417.

Herrera, G. A. 1992. Ultrastructural immunolabeling: a general overview of techniques and applications. Ultrastruct. Pathol. 16:37–45.

Horber, J. K. H., W. Haberle, F. Ohnesorge, G. Binnig, H. G. Liebich, C. P. Czerny, H. Mahnel, and A. Mayr. 1992. Investigation of living cells in the nanometer regime with the scanning force microscope. Scanning Microsc. 6:919–930.

Horisberger, M. 1979. Evaluation of colloidal gold as a cytochemical marker for transmission and scanning electron microscopy. *Biol. Cell.* 36:253–258.

Keller, D. J., and C. Chih-Chung. 1992. Imaging steep, high structures by scanning force microscopy with electron beam deposited tips. *Surface Sci.* 268:333–339.

Lacapere, J. J., D. L. Stokes, and D. Chatenay. 1992. Atomic force microscopy of three-dimensional membrane protein crystals. *Biophys J.* 63: 303–308.

Lee, K. L., D. W. Abraham, F. Secord, and L. Landtein. 1991. Submicron Si trench profiling with an electron-beam fabricated atomic force microscope tip. *J. Vac. Sci. Technol. B.* 9:3562–3568.

Loftus, J. C., and R. M. Albrecht. 1984. Redistribution of the fibrinogen receptor of human platelets following surface activation. *J. Cell Biol.* 99:822–829.

Marchant, R. E., S. A. Leas, J. D. Andrade, and P. J. Bockenstedt. 1992. Interactions of von Willebrand factor on mica studied by atomic force microscopy. *J. Colloid Interface Sci.* 148:261–272.

Mosher, D. F. 1975. Cross-linking of cold insoluble globulin by fibrin-stabilizing factor. *J. Biol. Chem.* 250:6614–6621.

Murthy, K. D., A. R. Diwan, S. R. Simmons, R. M. Albrecht, and S. L. Cooper. 1987. Utilization of immunogold labeling to compare the adsorption behavior of fibrinogen, fibronectin and albumin on polymers. *Scanning Microsc.* 1:765–773.

Olorundare, O. E., S. R. Simmons, and R. M. Albrecht. 1993. Evidence for two mechanisms of ligand-receptor movement on surface-activated platelets. *Eur. J. Cell Biol.* 60:131–145.

Park, K., R. M. Albrecht, S. R. Simmons, and S. L. Cooper. 1986. A new approach to study adsorbed proteins on biomaterials: immunogold staining. *J. Colloid Interface Sci.* 111:197–212.

Park, K., S. R. Simmons, and R. M. Albrecht. 1987. Surface characterization of biomaterials by immunogold staining–quantitative analysis. *Scanning Microsc.* 1:339–350.

Parpura, V., P. G. Haydon, and E. Henderson. 1993. Three-dimensional imaging of living neurons and glia with the atomic force microscope. *J. Cell Sci.* 104:427–432.

Pawley, J. B., and R. M. Albrecht. 1988. Imaging colloidal gold labels in LVSEM. *Scanning.* 10:184–189.

Putman, C. A. J., B. G. de Grooth, P. K. Hansma, N. F. van Hulst, and J. Greve. 1993. Immunogold labels: cell-surface markers in atomic force microscopy. *Ultramicroscopy.* 48:177–182.

Roth, J. 1983. The colloidal gold marker system for light and electron microscopic cytochemistry. *In* Techniques in Immunocytochemistry, Vol.2. C. G. R. Bullock and P. Petrusz, editors. Academic Press, New York. 217.

Shaiu, W., D. D. Larson, J. Vesenka, and E. Henderson. 1993. Atomic force microscopy of oriented linear dna molecules labeled with 5 nm gold sphere. *Nucleic Acids Res.* 21:99–103.

Simmons, S. R., and R. M. Albrecht. 1989. Probe ligand bound label conformation in colloidal gold-ligand labels and gold immunolabels. *Scanning Mircrosc.* 3(Suppl.):27s–34s.

Simmons, S. R., J. B. Pawley, and R. M. Albrecht. 1990. Optimizing parameters for correlative immunogold localization by video-enhanced light microscopy, high-voltage transmission electron microscopy, and field emission scanning electron microscopy. *J. Histochem. Cytochem.* 38: 1781–1785.

Stirling, J. W. 1990. Immuno- and affinity probes for electron microscopy: a review of labeling and preparation techniques. *J. Histochem. Cytochem.* 38:145–157.

Thundat, T., X.-Y. Zheng, S. L. Sharp, D. P. Allison, R. J. Warmack, D. C. Joy, and T. L. Ferrell. 1992. Calibration of atomic force microscope tips using biomolecules. *Scanning Microsc.* 6:903–910.

Vesenka, J., S. Manne, R. Giberson, T. March, and E. Henderson. 1993. Colloidal gold particles as an incompressible atomic force microscope imaging standard for assessing the compressibility of biomolecules. *Biophys. J.* 65:992–997.

Weisel, J. W., N. Chandrasekaran, G. Vilaire, and J. S. Bennett. 1992. Examination of the platelet membrane glycoprotein IIb-IIIa complex and its interaction with fibrinogen and other ligands by electron microscopy. *J. Biol. Chem.* 267:16637–16643.

Weisenhorn, A. L., B. Drake, C. B. Prater, S. A. Gould, P. K. Hansma, F. Ohnesorge, M. Egger, S. P. Heyn, and H. E. Gaub. 1990. Immobilized proteins in buffer imaged at molecular resolution by atomic force microscopy. *Biophys. J.* 58:1251–1258.